# Antisense-mediated loss of calcium homoeostasis endoplasmic reticulum protein (CHERP; ERPROT213-21) impairs $Ca^{2+}$ mobilization, nuclear factor of activated T-cells (NFAT) activation and cell proliferation in Jurkat T-lymphocytes

Flavia A. O'ROURKE[1], Janice M. LaPLANTE† and Maurice B. FEINSTEIN

Department of Pharmacology, University of Connecticut Health Center, Farmington CT, 06030, U.S.A., and †Division of Endocrinology, Diabetes and Hypertension, Brigham and Women's Hospital, Harvard Medical School, 221 Longwood Avenue, Boston, MA 02115, U.S.A.

We recently discovered a novel gene on chromosome 19p13.1 and its product, an integral endoplasmic reticulum (ER) membrane protein, termed CHERP (calcium homoeostasis endoplasmic reticulum protein). A monoclonal antibody against its C-terminal domain inhibits $Ins(1,4,5)P_3$-induced $Ca^{2+}$ release from ER membrane vesicles of many cell types, and an antisense-mediated knockdown of CHERP in human erythroleukemia (HEL) cells greatly impaired $Ca^{2+}$ mobilization by thrombin. In the present paper, we explore further CHERP's function in Jurkat T-lymphocytes. Confocal laser immunofluorescence microscopy showed that CHERP was co-localized with the $Ins(1,4,5)P_3$ receptor throughout the cytoplasmic and perinuclear region, as previously found in HEL cells. Transfection of Jurkat cells with a *lac*I-regulated mammalian expression vector containing CHERP antisense cDNA caused a knockdown of CHERP and impaired the rise of cytoplasmic $Ca^{2+}$ (measured by fura-2 acetoxymethyl ester fluorescence) caused by phytohaemagglutinin (PHA) and thrombin. A 50 % fall of CHERP decreased the PHA-induced rise of the cytoplasmic free $Ca^{2+}$ concentration ($[Ca^{2+}]_i$), but $Ca^{2+}$ influx was unaffected. Greater depletion of CHERP ($> 70$ %) did not affect the concentration of $Ins(1,4,5)P_3$ receptors, but diminished the rise of $[Ca^{2+}]_i$ in response to PHA to $\leqslant 30$ % of that in control cells, decreased $Ca^{2+}$ influx and slowed the initial rate of $[Ca^{2+}]_i$ rise caused by thapsigargin, an inhibitor of the sarcoplasmic/endoplasmic-reticulum $Ca^{2+}$-ATPase, suggesting there was also some deficit in ER $Ca^{2+}$ stores. In CHERP-depleted cells the $Ca^{2+}$-dependent activation and translocation of the key transcription factor NFAT (nuclear factor of activated T-cells) from cytoplasm to nucleus was suppressed. Furthermore, cell proliferation was greatly slowed (as in HEL cells) along with a 60 % decrease in cyclin D1, a key regulator of progression through the $G_1$ phase of the cell cycle. These findings provide further evidence that CHERP is an important component of the ER $Ca^{2+}$-mobilizing system in cells, and its loss impairs $Ca^{2+}$-dependent biochemical pathways and progression through the cell cycle.

Key words: cyclin D1, fura-2, $Ins(1,4,5)P_3$ receptor, thapsigargin, phytohaemagglutinin, RNA polymerase II.

## INTRODUCTION

We discovered a novel human gene located on chromosome 19p13.1 and its protein product, an integral endoplasmic reticulum (ER) membrane protein, that appears to be a new component of the $Ca^{2+}$ regulatory system in cells [1]. An approx. 4.0 kb cDNA was isolated from a human erythroleukaemia (HEL) cell cDNA expression library using a monoclonal antibody (mAb213-21) that we developed. This antibody was used in the screen because it inhibited $Ins(1,4,5)P_3$-induced $Ca^{2+}$ release from highly purified isolated ER membrane vesicles of several cell types, but did not react with the $Ins(1,4,5)P_3$ receptor. Additional clones that were isolated from human cerebellar and cardiac cDNA libraries and a human genomic foetal liver library were identical with the HEL cell cDNA in the regions sequenced. A corresponding mRNA transcript was present in all human cell lines and tissues examined. We designated this protein as CHERP (calcium homoeostasis endoplasmic reticulum protein; also known as ERPROT213-21;

GenBank® accession number U94836). By using a computer search, we found that Imbert et al. [2] had earlier reported a 1.8 kb cDNA sequence (i.e. DAN16; GenBank® accession number NM_006387) as part of an antibody screen of cDNA expression libraries for proteins with polyglutamine tracts that might be involved in spinocerebellar ataxia. DAN16 was identical with the 5′ end of CHERP, but was extended by 39 nt. We deduced the N-terminal sequence of CHERP protein by PCR amplification of HEL cell cDNA with a forward primer derived from the genomic sequence of CHERP in the region previously predicted by primer extension to be the transcript start site. The sequence was later verified by sequencing of a uterine leiomyosarcoma clone by R. Strausberg (GenBank® accession number BC021294). CHERP has a unique cDNA and amino acid sequence [1] and the genomic sequence is in GenBank® under accession number AC008764.9 (see http://greengenes.llnl.gov/mouse/html/parm.html).

The inhibition of $Ins(1,4,5)P_3$-induced release of $Ca^{2+}$ from isolated ER vesicles by mAb213-21 was reversed by $K^+$ ionophores

[3], which suggested that CHERP might be involved in the regulation of an ER transmembrane $K^+$ current, although there is no direct evidence at the present time that CHERP is an ER channel or a regulator of a channel. $K^+$ influx into the ER could operate as a countercurrent to the $Ca^{2+}$ efflux caused by $Ins(1,4,5)P_3$ so as to prevent the build-up of an ER transmembrane potential that would oppose $Ca^{2+}$ release [4]. It was also proposed that $K^+$ may displace bound $Ca^{2+}$ from ion-exchange storage proteins within the ER lumen, thereby increasing the pool of free $Ca^{2+}$ that could be released through open $Ins(1,4,5)P_3$ receptor channels [5].

To test the hypothesis that CHERP is involved in intracellular $Ca^{2+}$ homoeostasis in intact cells, we depleted the protein in the HEL cell line by transfecting cells with plasmids that produced *lac*I-regulated expression of CHERP antisense cDNA. Treatment of the antisense-transfected HEL cells with isopropyl $\beta$-D-thio-galactoside (IPTG), to relieve *lac*I repression, led to an approx. 80 % decline in CHERP over a 4-day period, with markedly decreased intracellular $Ca^{2+}$ mobilization evoked by thrombin, decreased DNA synthesis and growth arrest. These findings implied that CHERP has an important role in $Ca^{2+}$ homoeostasis and cell proliferation. Conversely, overexpression of CHERP, by transfection with a vector containing CHERP sense cDNA, enhanced the degree and duration of the cytoplasmic free $Ca^{2+}$ concentration ($[Ca^{2+}]_i$) response to thrombin. In further support of the hypothesis, immunofluorescence confocal microscopy demonstrated that CHERP was co-localized with the $Ins(1,4,5)P_3$ receptor in HEL cells [1].

To explore further the biological significance of CHERP, we chose to investigate the effects of its depletion on the Jurkat T-lymphocyte cell line as a model system with known $Ca^{2+}$-dependent functions. A rise of $[Ca^{2+}]_i$ is an early and critical event in the activation of the immune cells that are responsible for cellular and humoral immunity [6,7] and defective $[Ca^{2+}]_i$ mobilization or influx in humans has been associated with deficient immune-cell function [8,9]. T-cell activation is impaired by knockout of the $Ins(1,4,5)P_3$ receptor [10] involved in intracellular $Ca^{2+}$ release, and also when $Ca^{2+}$ entry is reduced by certain mutations in the Jurkat cell line [11] or by the HIV envelope protein gp160 [12].

$Ca^{2+}$ signals in T-cells can be very complex, varying in frequency, intensity and duration, and these variations in signalling patterns affect the expression of different genes and cell functions [13,14]. The regulation of intracellular $Ca^{2+}$ requires the co-ordinated function of many proteins, such as $Ins(1,4,5)P_3$ receptors, sarcoplasmic/endoplasmic reticulum $Ca^{2+}$-ATPases (SERCAs), and the plasma membrane $Ca^{2+}$-release-activated $Ca^{2+}$ (CRAC) channels, plasma membrane $Ca^{2+}$-ATPases (PMCAs), $Na^+/Ca^{2+}$ exchangers and $K^+$ channels, as well as mitochondrial pumps/exchangers and various kinases that regulate receptors and channels [13]. An early response of T-cells to their interaction with mitogens, lectins that activate the T-cell receptor (TCR), integrins or antigen peptide–MHC complexes is the activation of $Ca^{2+}$ release from intracellular stores [15]. This results from activation of protein tyrosine kinases leading to the downstream stimulation of phospholipase C$\gamma$, which generates $Ins(1,4,5)P_3$ and diacylglycerol from the hydrolysis of the membrane substrate $PtdIns(4,5)P_2$. $Ins(1,4,5)P_3$, acting on its receptors in the ER membrane, releases ER stores of $Ca^{2+}$ [10]. Furthermore, in T-cells, a biphasic increase in $[Ca^{2+}]_i$ results because the initial rapid $Ca^{2+}$ release from the ER then initiates a much larger rise of $[Ca^{2+}]_i$ owing to an influx of $Ca^{2+}$ from the extracellular space through so-called store-operated $Ca^{2+}$ channels (SOCs) to produce what is termed capacitive $Ca^{2+}$ entry [13]. These channels in the plasma membrane produce a CRAC current termed $I_{CRAC}$, a mechanism

for receptor-activated $Ca^{2+}$ entry into cells [16]. Ryanodine receptors in the ER, responding to the second messenger cADP-ribose, may also have a role in maintaining sustained $Ca^{2+}$ signals in human Jurkat T-cells and murine T-lymphoma cells [17], since the elevation of $Ins(1,4,5)P_3$ levels may be transient compared with $Ca^{2+}$ influx. On the other hand, lymphocytes appeared to be unaffected in mice lacking the ryanodine 3 receptor [18].

The regulation of intracellular $Ca^{2+}$ affects the ultimate response of an immune cell because $Ca^{2+}$ has a vital role in signal-transduction pathways, such as the activation of specific transcription factors, including nuclear factor $\kappa$B, activating protein 1 and nuclear factor of activated T-cells (NFAT), that are necessary for the expression of certain cytokines and cytokine receptors [19]. The elevation of $[Ca^{2+}]_i$ is an essential trigger for T-cell expression of interleukin-2 (IL-2) that is secreted by mitogen- or antigen-activated helper T-lymphocytes. IL-2 acts as an autocrine factor stimulating the expansion of antigen-specific T-cells, and as a paracrine factor influencing the activity and differentiation of B-cells [20], natural killer cells and lymphocyte-activated killer cells [21]. IL-2 expression requires the $Ca^{2+}$-dependent activation of transcription factors of the NFAT family [22]. The $Ca^{2+}$/calmodulin-dependent phosphatase calcineurin causes rapid dephosphorylation of NFAT proteins, necessary for their translocation to the nucleus and for increased affinity for DNA.

In the present paper, we show that regulated antisense-mediated knockdown of CHERP in the Jurkat T-cell line greatly impaired $Ca^{2+}$ mobilization caused by stimulation of the TCR pathway with phytohaemagglutinin (PHA) and by stimulation of the G-protein-linked thrombin receptor. This effect was accompanied by inhibition of the $Ca^{2+}$-dependent translocation of NFAT from cytoplasm to nucleus, and slowed cell proliferation in association with a decrease in cyclin D1 concentration. In addition, immunofluorescence microscopy showed that CHERP was co-localized with the $Ins(1,4,5)P_3$ receptor in Jurkat T-cells. These findings provide further evidence that CHERP is an important component of the $Ca^{2+}$-regulatory system in cells.

## MATERIALS AND METHODS

### Establishment of empty vector (V)-Jurkat and antisense (AS)-Jurkat cell lines

We used the LacSwitch mammalian cDNA expression system (Stratagene, La Jolla, CA, U.S.A.) for the selective induction of RNA transcription of CHERP antisense cDNA with IPTG [1,23]. Jurkat cells (clone E-61; ATCC, Rockville, MD, U.S.A.) were cultured in RPMI 1640 medium containing 10 % (v/v) foetal bovine serum (FBS; Hyclone, Logan, UT, U.S.A.) and were then washed and placed in Hybrimax medium (Sigma, St. Louis, MO, U.S.A.) for transfection with plasmids. Cells were co-transfected for 24 h using calcium phosphate with an *Escherichia coli lac*I expression plasmid p3′SS containing a hygromycin-resistance gene plus either the empty inducible mammalian expression vector pOPRSVICAT containing a geniticin-resistance gene (Stratagene) or pOPRSVICAT with a 3.4 kb insert of the CHERP antisense cDNA plasmid pJLRSV213/$\Delta$CAG.AS [1]. To make the latter vector, the chloramphenicol acetyltransferase gene of pOPRSVICAT was replaced with the *Eco*RI fragment from plasmid 3.9 kb pJLBS213/3.9 inserted in the antisense orientation relative to the promoter. To eliminate inadvertent antisense knockout of other messages containing extended CAG trinucleotide repeats, the 533 nt *Sma*I fragment, which spanned the CAG repeat region of pJLBS213/3.9, was deleted (corresponding to nt 759–1292 of cDNA; NM_006387). Jurkat

cell clones were selected for their combined resistance to geniticin and hygromycin. All clones were analysed by quantitative immunofluorescence for their expression of *lac*I (rabbit anti-lacI polyclonal sera; Stratagene) and for CHERP protein (mAb213-21) before and after incubation with IPTG to relieve *lac*I repression, as described previously in [1]. Cells that expressed empty vector with the *lac*I repressor (no knockdown of CHERP by IPTG) were designated V-Jurkat cells, and those transfected with the *lac*I repressor and vector containing CHERP antisense cDNA (maximal IPTG-induced knockdown of CHERP protein concentration) were designated AS-Jurkat cells. Stable clonal lines were established by limiting dilution and maintained in the presence of 75 $\mu$g/ml hygromycin and 150 $\mu$g/ml geniticin. Cells were stored at early passage in liquid nitrogen and recloned periodically.

## Localization and quantification of proteins by immunofluorescence microscopy

Cells plated on to polylysine-coated coverslips were fixed in 4 % (v/v) formaldehyde in PBS for 15 min, followed by three washes with PBS. The fixed cells were permeabilized for 15 min with 200 $\mu$l of 0.1 % (v/v) Triton X-100 in PBS with 1 % (v/v) goat serum added and then washed twice. All antibodies were diluted in PBS with 0.1 % (v/v) goat serum and 0.02 % (v/v) Triton X-100. To assay single proteins, cells were incubated for an additional 1 h with one of the following antibodies: (i) mouse monoclonal anti-CHERP mAb213-21, freshly harvested and purified [3] from hybridoma cell cultures growing in the protein-free medium Hybrimax, diluted 1:20, (ii) polyclonal rabbit anti-[Ins(1,4,5)$P_3$ receptor] sera (Accurate Scientific, Westbury, NJ, U.S.A.), which recognizes receptor subtypes 1, 2 and 3, diluted 1:200, (iii) mouse monoclonal antibody 8WG16 (Covance, Richmond, CA, U.S.A.), which recognizes the C-terminal heptapeptide repeat on the largest subunit of RNA polymerase II, diluted 1:100, (iv) mouse monoclonal antibody against NFAT1 amino acids 29–181 (Transduction Laboratories, Lexington, KY, U.S.A.), diluted 1:100, and (v) mouse monoclonal antibody against cyclin D-1 (Transduction Laboratories), which recognizes the cyclin box, diluted 1:100. After incubation with an antibody, the cells were washed three times and were then incubated for an additional 1 h with the appropriate cyanin-3-conjugated AffiniPure F(ab′)$_2$ fragment goat anti-mouse IgG + IgM (heavy and light chains) or cyanin-3-conjugated goat anti-rabbit (heavy and light chains) secondary antibodies (Jackson Immunoresearch Laboratories, West Grove, PA, U.S.A.), diluted 1:500–1:800. CHERP was also detected using 1.0 mg of mAb213-21 that was directly labelled with FITC by the Quicktag conjugation kit (Boehringer Mannheim, Indianapolis, IN, U.S.A.) and diluted 1:100.

After all incubations with antibodies, the cells were washed three times in PBS and mounted with Prolong Antifade media (Molecular Probes, Eugene, OR, U.S.A.). Fluorescence images of cells were collected and analysed in two ways. One system used a SPOT camera (Version 1.1; Diagnostic Instruments, Sterling Heights, MI, U.S.A.) mounted on an Olympus fluorescence microscope 1 × 70 equipped with LCPlan Fluor 40× [numerical aperture (NA) 0.6] and UPlanApo 100 × oil/iris (NA 1.35) objectives, and mirror cube units with excitation filters for 4,6-diamidino-2-phenylindole (DAPI; Sigma; 360–370 nm), FITC (460–490 nm), and rhodamine or propidium iodide (530–550 nm) fluorescence. Fluorescence emission signals were quantified using the public domain National Institutes of Health (NIH) Image 1.61 image analysis software. The second system consisted of an Olympus 1 × 70 fluorescence microscope equipped with

a Hamamatsu ORCA-ER digital camera. The acquisition and analysis of fluorescence images of cells was accomplished by Improvision Openlab 3 software running on a Macintosh Powermac G4 dual microprocessor computer. Fluorescence units for individual cells were calculated as the mean fluorescence pixel intensity (minus the mean background level) multiplied by the cell area in square pixels. Each cell area was delineated as a region of interest by OpenLab 3 software. The summed fluorescence units ($\times 10^{-5}$, for simplicity) of all cells in an assay was divided by the total number of cells analysed, and reported as the mean ($F_{mean}$) $\pm$ S.E.M. of the population. Statistical analysis using Student's *t* test was performed using Sigmaplot 4.0 software. A statistically significant difference between population means was assumed at $P < 0.05$.

To study the intracellular localization of the Ins(1,4,5)$P_3$ receptor and CHERP, we fixed and permeabilized Jurkat cells, as described above, and incubated them with FITC-labelled mAb213-21 and with polyclonal rabbit anti-[Ins(1,4,5)$P_3$ receptor] sera, followed by detection of the latter with cyanin-3-labelled secondary antibody, as previously described in [1]. Fluorescence was viewed with a Zeiss LSM410 laser confocal microscope with a Zeiss Plan Apochromat × 63 NA 1.4 oil lens in the Center for Biological Imaging (University of Connecticut Health Center). Two-colour overlays of merged images were assembled using Adobe Photoshop 4.0 software. For controls, cells were also incubated with secondary antibodies alone to measure non-specific binding, and with a CHERP-derived glutathione S-transferase (GST) fusion protein that blocks mAb213-21 binding to CHERP with an IC$_{50}$ of 0.7 $\mu$M. The GST fusion protein, comprising the 2.6 kDa domain from Pro⁴¹⁷ to the C-terminus of CHERP, was isolated after being expressed in *E. coli* using CHERP cDNA plasmid pJLBS213/2.6 cloned in-frame into pGEX-5 × 1 (Amersham Biosciences, Piscataway, NJ, U.S.A.) to make plasmid pJLGST213/2.6 [1].

## Measurement of [Ca²⁺]ᵢ with fura-2 acetoxymethyl ester (fura-2/AM)

Jurkat cell [Ca²⁺]ᵢ was measured in individual cells by fluorescence microscopy, and in cell suspensions by spectrofluorimetry. For fluorescence microscopy AS-Jurkat cells (approx. 10⁵ cells/ml) growing in RPMI 1640 containing 10 % (v/v) FBS, untreated or treated with IPTG for up to 4 days, were plated on to polylysine-coated cover slips and were pre-incubated for 1 h at 37 °C. The cells were loaded with fura-2/AM, as previously described in [1,23] with the following modifications: cells were washed with Hepes phosphate saline solution (HPSS) containing 1.8 mM Ca²⁺ and were incubated with 5 $\mu$M fura-2/AM at room temperature (21–23 °C) for 45 min followed by washing with HPSS containing 1.0 % (v/v) BSA to remove fura-2/AM. Cells were then washed and maintained for an additional 1 h in Hybrimax (containing 0.5 mM Ca²⁺) before mounting the cover slips into a chamber with 300 $\mu$l of HPSS containing 0.5 mM Ca²⁺. HPSS (600 $\mu$l), containing appropriate concentrations of PHA, thapsigargin or cyclopiazonic acid, was added to the chamber to release internal calcium stores in the cells. The fura-2/AM-loaded cells were viewed with an Olympus 1 × 70 fluorescence microscope with a Nikon Fluor 100 × 1.3 NA inverted oil immersion lens as part of an IonOptix Imaging System (Milton, MA, U.S.A.). Microscopic fields were flashed alternately at a rate of 1 Hz with excitation light at wavelengths of 340 nm and 380 nm and fluorescence emission was measured at 510 nm [24]. Image data were collected from outlined rectangular zones surrounding individual cells and background areas (for

subtraction) in a microscopic field, as previously employed in [1,23]. The data were collected and analysed to calculate $[Ca^{2+}]_i$ using IonWizard and IMGACQ software (IonOptix). Cellular autofluorescence, measured (510 nm emission) in the absence of fura-2/AM, was undetectable at the exposure times and gain used to obtain images in fura-2/AM-loaded cells, and was unchanged by the addition of PHA.

$[Ca^{2+}]_i$ was also measured in Jurkat cell suspensions with a Hitachi F-2000 spectrofluorimeter. Fura-2/AM-loaded cells (approx. $1.2 \times 10^6$ cells/ml) in Hybrimax (0.5 mM $Ca^{2+}$) were magnetically stirred at 21–22 °C in a 1.0 ml cuvette. The fluorescence emission at 510 nm was recorded on a personal computer at excitation wavelengths of 340 and 380 nm. $[Ca^{2+}]_i$ was calculated from the 340/380 ratio, using a $K_D$ of 224 nM for the fura-2/AM–$Ca^{2+}$ complex, as described by Grynkiewicz et al. [25]. $R_{max}$ and $R_{min}$ were determined in medium containing 0.5 mM $Ca^{2+}$ by lysing cells with 0.5 % (v/v) Triton X-100 for $R_{max}$, followed by addition of excess EGTA to obtain $R_{min}$. Autofluorescence (510 nm emission) of cells not loaded with fura-2/AM was undetectable at the same spectrofluorimeter gain used to measure $[Ca^{2+}]_i$ in fura-2/AM-loaded cells, and was not affected by stimulation of cells with PHA. In some experiments, aliquots of the cell suspensions used to measure $[Ca^{2+}]_i$ were assayed for CHERP content by immunofluorescence microscopy.

### NFAT translocation to the nucleus

AS-Jurkat cells and AS-Jurkat cells (approx. $10^5$ cells/ml) treated with 10 $\mu$M IPTG for 4 days were washed with Hybrimax. The cells were plated onto polylysine-coated coverslips for 5 min at 37 °C, followed by washing with Hybrimax. Incubation medium containing either 10 nM thrombin or 10 $\mu$g/ml PHA was added to activate the $Ins(1,4,5)P_3$ pathway. The calcineurin antagonist cyclosporin (1 $\mu$M), which inhibits dephosphorylation of cytoplasmic NFAT and its translocation from cytoplasm to nucleus, was used as a negative control to block the response to thrombin and PHA. Addition of EGTA (4 mM) to the medium to chelate extracellular $Ca^{2+}$ and prevent its influx into cells was used as another negative control. To activate calcineurin, ionomycin (2 $\mu$M), which permits direct entry of $Ca^{2+}$ into the cell, bypassing the $Ins(1,4,5)P_3$ pathway, was used as a positive control. The cells were stimulated with thrombin or PHA for 15 min at 37 °C, then washed with PBS, fixed in 1 ml of 10 % (v/v) formaldehyde in PBS for 15 min, and then washed three times with PBS. The cells were then permeabilized for 15 min with 200 $\mu$l of 0.1 % (v/v) Triton X-100 in PBS containing 1 % (v/v) goat serum, washed twice, and finally incubated for 1 h with monoclonal antibody against NFAT1 amino acids 29–181, at 1:100 dilution and then for 1 h with cyanin-3-conjugated goat anti-mouse secondary antibody, diluted 1:500. Cells were then washed and treated with the selective nuclear stain DAPI for 5 min in the dark, washed with water and mounted with Prolong Antifade medium (Molecular Probes) for viewing in the microscope with a SPOT camera to obtain digital colour images.

### Assays for cell proliferation, viability, senescence and apoptosis

Proliferation of AS-Jurkat cells, in the presence or absence of IPTG, was measured over a period of 4 days by direct counting of viable cells (Trypan Blue exclusion) in an American Optical haemocytometer, and also by the CellTiter 3-(4,5-dimethyl-thiazol-2-yl)-2,5-diphenyl-2$H$-tetrazolium bromide ('MTT') cell proliferation assay (Promega, Madison, WI, U.S.A.), according to the manufacturer's instructions. AS-Jurkat cells ($10^6$ cell/ml),

untreated or treated for 1–4 days with 20 mM IPTG, were plated onto polylysine-coated coverslips and were washed, fixed and assayed for nuclear staining of senescence-associated $\beta$-galactosidase activity [26], as previously described in [1]. The DeadEnd™ Fluorimetric terminal deoxynucleotidyl transferase-mediated dUTP nick-end labelling (TUNEL) system (Promega) was used to measure the fragmented DNA of apoptotic cells on cover slips by catalytically incorporating fluorescein-12-dUTP at 3′-OH DNA ends using the enzyme terminal deoxynucleotidyl transferase, which forms a polymeric tail. The fluorescein-12-dUTP-labelled DNA was visualized directly using fluorescence microscopy as green nuclear fluorescence against a red nuclear background due to propidium iodide.

## RESULTS

### Co-localization of CHERP and Ins(1,4,5)$P_3$ receptor in Jurkat cells

Immunofluorescence microscopy using FITC–mAb213-21, and with mAb213-21 plus a cyanin-3-labelled secondary antibody, showed that CHERP was distributed throughout the cytoplasmic and perinuclear region, similar to the distribution of the $Ins(1,4,5)P_3$ receptor (Figure 1). Double labelling with FITC–mAb213-21 (green) and $Ins(1,4,5)P_3$ receptor antiserum plus cyanin-3-labelled secondary antibody (red) resulted in a yellow punctate fluorescence throughout the cytoplasm and perinuclear region owing to overlap of the red and green signals. This indicates that the two proteins are co-localized, presumably in the ER membranes of the Jurkat cells, as we previously observed in HEL cells [1].

### Knockdown of CHERP protein by stable transfection of Jurkat cells with antisense cDNA

We employed the same strategy that we previously used to produce effective knockdown of CHERP and GTPase-activating protein GAP1$^{IP4BP}$ in HEL cells [1,23]. Jurkat cell lines transfected with *E. coli lac*I, using the LacSwitch mammalian transfection system, were co-transfected with either an empty inducible mammalian expression vector pOPRSVICAT (V-Jurkat), or pOPRSVICAT with a 3.4 kb insert of CHERP antisense cDNA (AS-Jurkat). LacI blocks transcription by binding to the *lac* operator, which is embedded in the promoter of the CHERP antisense expression vector pJLRSV213/ΔCAG.AS. IPTG decreases the binding of lacI protein to the operator sequences, triggering transcription of the CHERP antisense cDNA. The lacI-regulated expression of CHERP antisense cDNA has the virtue that cells transfected with both vectors, but not treated with IPTG, serve as controls for the non-specific effects of transfection without depletion of CHERP. Furthermore, wild-type cells were treated with IPTG to control for any non-specific effects.

Three Jurkat clones transfected with CHERP antisense plasmid had high resistance to both geniticin and hygromycin, indicating that they contained both *lac*I and the CHERP antisense vector. These cells showed no decrease in CHERP content compared with wild-type or V-Jurkat cells, but incubation with IPTG produced a time- and dose-dependent reduction in the concentration of CHERP as measured by immunofluorescence microscopy. IPTG had no significant effect on CHERP content in wild-type Jurkat cells or in V-Jurkat cells. The clone showing the greatest reduction of CHERP by IPTG was selected for further characterization, and was designated as the AS-Jurkat cell line. AS-Jurkat cells were exposed to various concentrations of IPTG (5–25 mM) for 1–5 days to determine the optimal concentrations and times to use for knockdown of CHERP protein. The concentration of IPTG used in various experiments was adjusted according to the concentration
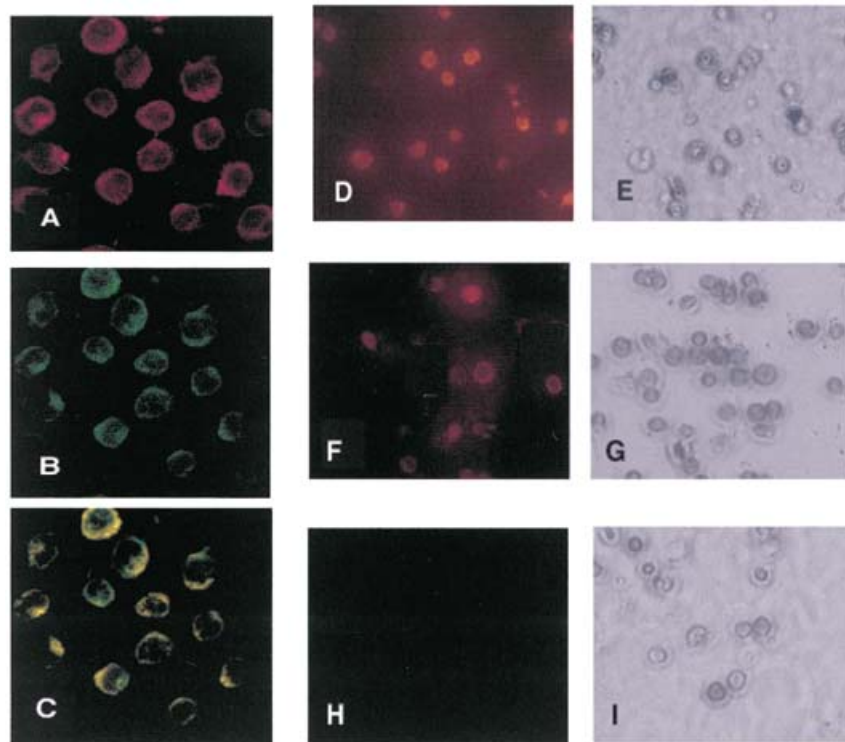
**Figure 1   Immunolocalization of CHERP and the Ins(1,4,5)$P_3$ receptor in Jurkat cells**

(**A**) The Ins(1,4,5)$P_3$ receptor was detected with polyclonal rabbit anti-[Ins(1,4,5)$P_3$ receptor] sera, which recognizes receptor subtypes 1,2, and 3, plus cyanin-3-labelled secondary antibody (red). (**B**) FITC-labelled mAb213-21 was used to detect CHERP (green). (**C**) A two-colour overlay of double-labelled cells showing co-localization of CHERP and the Ins(1,4,5)$P_3$ receptor (yellow). (**D**)–(**I**) Knockdown of CHERP in AS-Jurkat cells treated with IPTG. (**D**), (**F**) and (**H**) are immunofluorescence images of CHERP detected with mAb213-21 and cyanin-3-labelled secondary antibody. (**E**), (**G**) and (**I**) are the corresponding phase-contrast images. (**D**) and (**E**) Normal CHERP immunofluorescence in untreated AS-Jurkat cells. (**F**) and (**G**) CHERP in AS-Jurkat cells treated with 12.5 mM IPTG for 4 days. In IPTG-treated cells, the CHERP $F_{mean}$ was $1.159 \pm 0.069$, compared with an $F_{mean}$ of $4.485 \pm 0.051$ in cells in the absence of IPTG ($n = 65$; $P < 0.01$). The $F_{mean}$ for the Ins(1,4,5)$P_3$ receptor in control AS-Jurkat cells was $1.149 \pm 0.12$ ($n = 58$), compared with $1.109 \pm 0.07$ for IPTG-treated cells ($n = 43$), a difference that was not statistically significant ($P = 0.76$). (**H**) and (**I**) The presence of a GST fusion protein comprising the 2.6 kDa CTD of CHERP blocks the detection of CHERP, demonstrating the specificity of mAb213-21.

of cells used. Figures 1(D)–1(I) show representative microscopic fields with fluorescence and phase-contrast images from a typical experiment in which treatment of AS-Jurkat cells with 12.5 mM IPTG for 4 days caused a 74 % decline in the mean CHERP content (see legend, Figure 1). CHERP immunofluorescence in approx. 80 % of IPTG-treated cells was below that of the lowest control cell, and their mean CHERP content was only 20 % of that of the mean for control cells. The remaining 20 % of IPTG-treated AS-Jurkat cells had CHERP immunofluorescence within the lower half of the normal range of control AS-Jurkat cells (i.e. mean = 41 % of controls). This is not unexpected, since the concentration of IPTG was not maximal for knockdown of CHERP. The Ins(1,4,5)$P_3$ receptor content, measured in the same batch of cells, was unchanged (see legend, Figure 1). Therefore, in the population of cells that had only 26 % of the normal CHERP content, there was no significant loss of Ins(1,4,5)$P_3$ receptors.

## Ca$^{2+}$ mobilization is impaired in CHERP-depleted AS-Jurkat cells

[Ca$^{2+}$]$_i$ was monitored by ratiometric fluorescence microscopy of fura-2/AM-loaded Jurkat cells stimulated with PHA or thrombin, which both activate phospholipase C to produce the Ins(1,4,5)$P_3$ that releases intracellular Ca$^{2+}$ stores from the ER in Jurkat cells. The mitogenic lectin PHA stimulates TCR pathways, and thrombin acts via a G-protein-coupled receptor [27]. Emptying of ER Ca$^{2+}$ stores triggers a large sustained influx of extracellular

Ca$^{2+}$ through plasma membrane calcium channels that raises [Ca$^{2+}$]$_i$ to much higher levels than can be attained solely from the intracellular stores. We did not attempt to selectively isolate intracellular Ca$^{2+}$ release from influx by chelating extracellular Ca$^{2+}$ as we did in HEL cells [1], or with influx inhibitors, since ER calcium stores in T-cells are rapidly lost when refilling of stores via influx is prevented [13]. Therefore, unless stated otherwise, all experiments were conducted with 0.5 mM Ca$^{2+}$ in the medium so that fura-2/AM fluorescence is a measure of both intracellular release and influx.

We first measured fura-2/AM ratios by fluorescence microscopy in individual cells adherent to coverslips. Cells were stimulated with 20 $\mu$g/ml PHA and the 340/380 nm fura-2/AM fluorescence ratio was recorded for individual cells' microscopic fields over a period of 400–500 s, and [Ca$^{2+}$]$_i$ was calculated as previously described in [1,23]. In a typical experiment, the mean baseline [Ca$^{2+}$]$_i$ of AS-Jurkat cells was $53 \pm 5$ nM, which increased to a peak of $107 \pm 9.4$ nM ($n = 25$) when cells treated with IPTG for 4 days were stimulated with PHA. In control AS-Jurkat cells, [Ca$^{2+}$]$_i$ rose from the same baseline to $441 \pm 169$ nM ($n = 27$; $P = 0.013$), a net 7.2-fold greater response than in cells with a knockdown of CHERP. The population statistics showed that 70 % of PHA-stimulated IPTG-treated cells had a peak rise of [Ca$^{2+}$]$_i$ below that of the lowest control cell. The other 30 % of IPTG-treated cells had responses mostly within the lower end of the normal range of response to PHA, and may correspond to the cells with the least knockdown of CHERP (Figure 1).

Subsequent studies on stirred cell suspensions in a spectrofluorimeter cuvette showed that the $Ca^{2+}$-mobilizing effect of PHA in wild-type Jurkat cells was unaffected by their transfection with CHERP-antisense vector (AS-Jurkat cells) in the absence of IPTG, whereas the dose–response to PHA was depressed in AS-Jurkat cells treated with IPTG for 4 days (Figure 2a). $Ca^{2+}$ mobilization by thrombin was similarly inhibited (results not shown). Both the rate of rise of $[Ca^{2+}]_i$ and peak $[Ca^{2+}]_i$ due to PHA were decreased in IPTG-treated cells. For example, the results shown in Figure 2(b) indicate a net maximal increase in $[Ca^{2+}]_i$ of $0.76\,\mu M$ for the control cells, but only $0.1\,\mu M$ for the IPTG-treated cells; a response that was only 13 % of that in control cells. Strikingly, the initial rate of rise of $[Ca^{2+}]_i$, which is due mainly to release of ER stores, was only 1 % of the rate in AS-Jurkat cells without IPTG. The mean CHERP content of that specific batch of IPTG-treated cells, measured by immunofluorescence microscopy, was only 28.4 % that of untreated cells (see legend, Figure 2). In a total of five experiments, using different batches of cells treated in the same way (CHERP was not measured in the other four), the mean peak elevation of $[Ca^{2+}]_i$ above baseline due to PHA was reduced by 70 % in IPTG-treated cells; i.e. mean increase of $0.59 \pm 0.07\,\mu M$ in control AS-Jurkat cells, and $0.18 \pm 0.04\,\mu M$ in IPTG-treated AS-Jurkat cells ($P < 0.05$).

The SERCA inhibitor thapsigargin was also used to directly release ER $Ca^{2+}$ stores and induce a further rise in $[Ca^{2+}]_i$ due to $Ca^{2+}$ influx by SOCs, largely attributed to CRAC [28]. Figure 2(c) shows a typical response to thapsigargin in IPTG-treated AS-Jurkat cells from the same batch used to obtain the results shown in Figure 2(b). In this experiment, the thapsigargin-induced rate of rise of $[Ca^{2+}]_i$ (i.e. $\mu M/s$) in the CHERP-depleted cells was initially only 25 % of the rate in the control cells. It subsequently increased 2.76-fold to attain 80 % of the maximal rate in control cells, possibly due to activation of CRAC channels by the rising $[Ca^{2+}]_i$ coming from the ER [29]. In three experiments, the mean thapsigargin-induced peak increase of $[Ca^{2+}]_i$ above basal levels in the CHERP-depleted cells was not significantly different from that in controls (see legend, Figure 2c), although the initial rate of rise of $[Ca^{2+}]_i$ was lower in each case. Significantly, the mean net increase of $[Ca^{2+}]_i$ caused by thapsigargin in IPTG-treated cells was 4-fold greater than the increase elicited by PHA in the same batches of cells; i.e. $0.72 \pm 0.19\,\mu M$, compared with $0.18 \pm 0.04\,\mu M$; $P < 0.05$. In the presence of SERCA inhibitors, the fall in $[Ca^{2+}]_i$ after initial release from the ER is solely due to transport by the PMCA [30]. The rate and extent of decline of $[Ca^{2+}]_i$ caused by adding EGTA to the medium at the peak of the response (results not shown), to arrest influx, indicated that CHERP-depleted cells cleared cytosolic $Ca^{2+}$ as well as control cells, indicating that they had normal PMCA activity.

Cells with a marked deficit in response to PHA were also used to indirectly evaluate $Ca^{2+}$ influx, which is due largely, if not entirely, to $I_{CRAC}$ [13,31–34]. Adding 1 mM EGTA at the peak of the PHA responses, to reduce extracellular $Ca^{2+}$ concentrations to virtually nothing, causes $[Ca^{2+}]_i$ to fall back to pre-stimulus levels. Restoring excess extracellular $Ca^{2+}$ (3 mM) causes a sharp rise of $[Ca^{2+}]_i$ due to influx, which serves as an indirect measure of CRAC current [12]. We evaluated $Ca^{2+}$ influx this way in a batch of IPTG-treated AS-Jurkat cells in which PHA increased $[Ca^{2+}]_i$ by a mean of only 31.7 % compared with controls (i.e. three experiments, mean increase of $[Ca^{2+}]_i = 0.2\,\mu M$ compared with $0.63\,\mu M$; $P < 0.05$). Restoring excess extracellular $Ca^{2+}$ after EGTA to the IPTG-treated, PHA-stimulated, cells produced a rise of $[Ca^{2+}]_i$ that was lower in rate and magnitude compared with that in control cells (i.e. mean net increase of $[Ca^{2+}]_i = 0.35$ compared with $1.33\,\mu M$; $P < 0.05$).
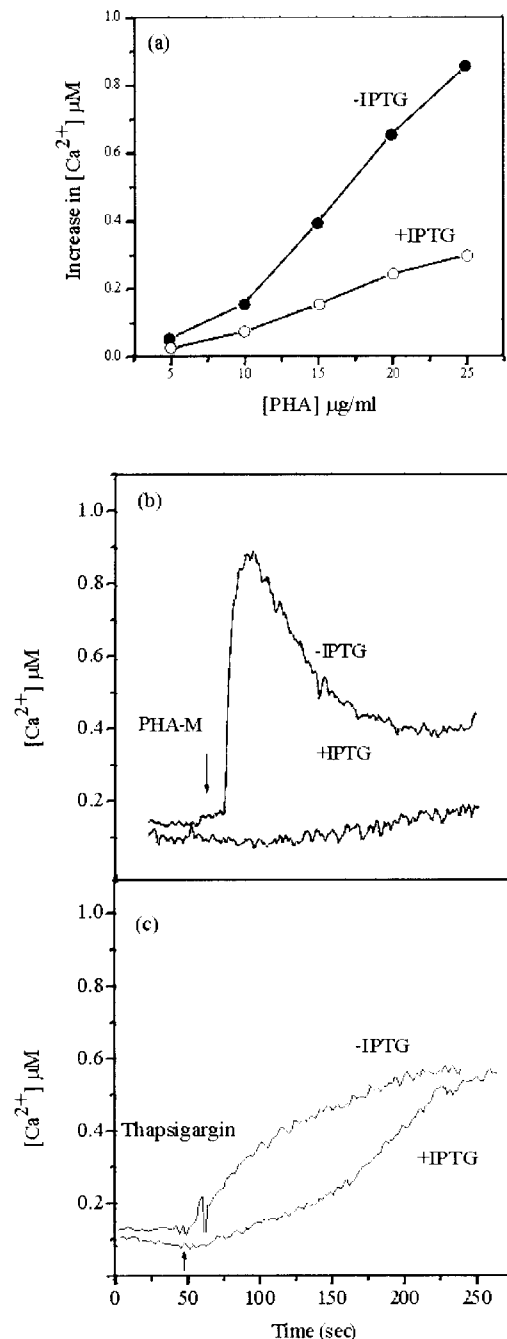


**Figure 2    $Ca^{2+}$ mobilization is impaired in CHERP-depleted Jurkat cells**

$[Ca^{2+}]_i$ was measured in stirred cell suspensions ($1.2 \times 10^6$ cells/ml) at room temperature in a spectrofluorometer, using fura-2/AM as a fluorescence indicator (see the Materials and methods section for details). Cells were loaded with fura-2/AM for 30 min at 37 °C, followed by washing with HPSS containing 0.1 % (v/v) BSA at room temperature and were incubated for a further 1 h before stimulation in a spectrofluorometer. To decrease CHERP expression, AS-Jurkat cells were incubated with 20 mM IPTG for 4 days. (**a**) Dose–response to PHA in control and IPTG-treated AS-Jurkat cells. Responses are the maximum $[Ca^{2+}]_i$ increases above baseline caused by PHA. Dose–responses were obtained on two additional batches of cells with similar results. (**b**) Response to PHA (20 $\mu$g/ml) in control and IPTG-treated AS-Jurkat cells. The baseline of control cells is shifted upward for clarity. (**c**) Response to thapsigargin (5 $\mu$M) in same batch of cells as used in (**b**). In three experiments, the mean thapsigargin-induced peak increase of $[Ca^{2+}]_i$ above baseline levels was $0.82 \pm 0.11\,\mu$M for controls compared with $0.72 \pm 0.19\,\mu$M for IPTG-treated cells ($P > 0.05$). The mean CHERP content of cells used in (**b**) and (**c**) was measured by immunofluorescence microscopy. IPTG-treated cells had 28.4 % of the CHERP content of control cells [an $F_{mean}$ of $1.85 \pm 0.26$ for IPTG-treated cells ($n = 75$) compared with $6.52 \pm 1.5$ for control cells ($n = 101$); $P < 0.05$].
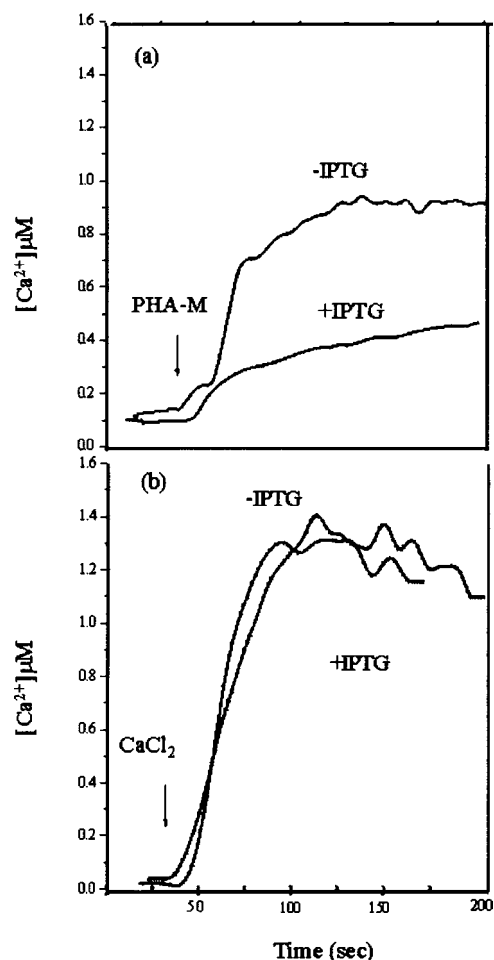
**Figure 3   PHA-induced Ca²⁺ mobilization and Ca²⁺ influx in AS-Jurkat cells with decreased geniticin resistance**

The mean CHERP content of IPTG-treated cells, determined by immunofluorescence microscopy, was 52 % of that in control cells. These cells had lost some geniticin resistance. $[Ca^{2+}]_i$ was measured as described in Figure 2. (**a**) Control AS-Jurkat cells (three experiments), and cells treated with 20 mM IPTG for 4 days (three experiments), were stimulated with 25 $\mu$g/ml PHA. The tracings show the mean responses. The difference in the mean peak increase above baseline of $0.80 \pm 0.04$ $\mu$M compared with $0.35 \pm 0.06$ $\mu$M is statistically significant ($P < 0.05$). (**b**) EGTA (1 mM) was added at 200 s, at the peak of the response to PHA in (**a**). $[Ca^{2+}]_i$ decreased back to baseline within 80 s (results not shown), at which time 3 mM Ca²⁺ was added to the medium as indicated by the arrow. The rise of $[Ca^{2+}]_i$ under these conditions (mean of three experiments for each condition) is due entirely to Ca²⁺ influx. There is no statistical difference between the peak responses ($P > 0.05$).

This result indicates that markedly defective mobilization of Ca²⁺ by PHA in CHERP-depleted Jurkat cells is also accompanied by decreased Ca²⁺ influx.

Over time, AS-Jurkat cells began to lose significant geniticin sensitivity and had to be recloned periodically to maintain cells with high antibiotic resistance and maximal knockdown of CHERP by IPTG. This provided the opportunity to test cells with lesser depletion of CHERP. Exposure of one batch of cells with partially lowered geniticin resistance to IPTG for 4 days decreased CHERP by only 52 %, and those cells proliferated at a nearly normal rate. The net peak rise of $[Ca^{2+}]_i$ above baseline caused by PHA was decreased by 56 % in IPTG-treated cells (see legend, Figure 3a). In contrast, the initial rate and the peak rise of $[Ca^{2+}]_i$ owing to Ca²⁺ influx in the same cells was unaffected (Figure 3b). The peak rise of $[Ca^{2+}]_i$ in response to thapsigargin
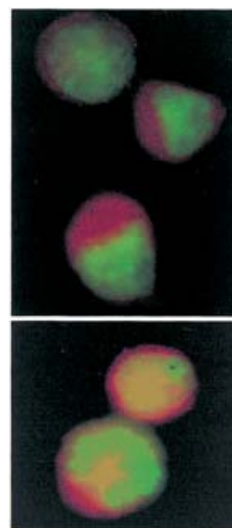


**Figure 4   Imaging of NFAT1 translocation to the nucleus in Jurkat cells**

NFAT1 was detected in fixed AS-Jurkat cells with a monoclonal antibody plus a cyanin-3-labelled anti-mouse secondary antibody (see the Materials and methods section). The nucleus was specifically labelled with DAPI, whose fluorescence emission was observed with a green FITC filter. The images are two-colour overlays of the cyanin-3 and DAPI signals. Upper panel: control cells (AS-Jurkat cells untreated with IPTG), showing the DAPI-stained (green) nucleus and NFAT1 (red) in the cytoplasm. Lower panel: control cells stimulated with PHA, showing yellow areas in the nuclei due to translocation of NFAT1 (red) into green DAPI-stained nuclei.

was also not significantly different in the same IPTG-treated and control cells (three experiments, results not shown), indicating that ER Ca²⁺ stores and CRAC current were probably normal. These data indicate that a partial loss of CHERP can impair release of Ca²⁺ stores by PHA even when ER Ca²⁺ stores and CRAC appear to be normal.

## CHERP knockdown inhibits translocation of NFAT1

We investigated the possibility that translocation of NFAT1 from the cytosol to the nucleus, which is a Ca²⁺/calcineurin-dependent signal transduction pathway [22], might be affected in CHERP-depleted AS-Jurkat cells. NFAT translocation to the nucleus is a definitive measure of its activation, and a more biologically relevant assay than the gel mobility shift used to measure dephosphorylation of the protein. Immunofluorescence microscopy using an antibody to NFAT1 showed the protein was confined to the cytoplasm of all unstimulated AS-Jurkat cells, clearly differentiated from the nucleus that was specifically stained with blue fluorescent DAPI (results not shown). Translocation of NFAT1 was measured by a new method, employing the FITC-detection filter to isolate the green fluorescence region of the emission spectrum of DAPI. Figure 4 (upper panel) shows unstimulated AS-Jurkat cells in which NFAT1 (red cyanin-3) is seen confined to the cytoplasm. In the absence of stimulation, virtually no cells were positive for NFAT1 in the nucleus. When AS-Jurkat cells (untreated with IPTG) were stimulated with PHA or thrombin to raise $[Ca^{2+}]_i$, the green DAPI-labelled nuclei of most cells became yellow due to the influx of NFAT1 (red; Figure 4, lower panel). We found that this two-colour fluorescence method provided a more precise identification of nuclear NFAT1 compared with using only an NFAT1 primary antibody detected with an FITC-labelled secondary antibody [35]. The response to PHA and thrombin was totally blocked by 5 $\mu$M cyclosporin or 2 mM EGTA, used
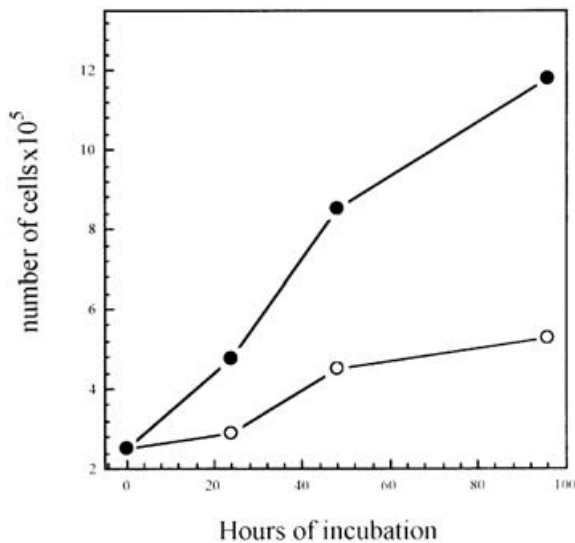
**Figure 5   Decreased cell proliferation in CHERP-depleted cells**

Aliquots of AS-Jurkat cell cultures, in the absence (●) or presence (○) of 20 mM IPTG, were stained with Trypan Blue and viable cells were counted using a haemocytometer. Results are representative of three experiments. In two additional experiments, the same result was obtained using the 3-(4,5-dimethylthiazol-2-yl)-2,5-diphenyl-2H-tetrazolium bromide ('MTT') assay to measure cell proliferation.

to inhibit calcineurin and $Ca^{2+}$ influx respectively (results not shown). The translocation of NFAT1 due to PHA and thrombin was blocked in most cells incubated with IPTG for 72 h to deplete CHERP. Stimulation of control AS-Jurkat cells by PHA caused yellow nuclei in 79 % of cells ($n=14$), which was reduced to 33 % yellow nuclei in cells treated with IPTG ($n=45$). A similar result was obtained with thrombin as the stimulus; i.e. 72 % of thrombin-stimulated AS-Jurkat cells ($n=32$) were positive for NFAT1 in the nucleus, which was reduced to 25 % in AS-Jurkat cells treated with IPTG ($n=36$). Therefore, the treatment of AS-Jurkat cells with IPTG caused an overall 62 % decrease in agonist-stimulated NFAT1 positive nuclei. In contrast, the treatment of AS-Jurkat cells (with or without IPTG) with 1 $\mu$M ionomycin, which directly causes the release of ER $Ca^{2+}$ stores and the influx of extracellular $Ca^{2+}$, resulted in NFAT1 translocation to the nucleus in all cells. Thus the decreased nuclear translocation of NFAT1 by agonists in CHERP-depleted AS-Jurkat cells is clearly attributable to defective mobilization of $Ca^{2+}$.

**Impaired proliferation and decreased cyclin D1 in CHERP-depleted Jurkat cells**

Stable transfection of the Jurkat cell line with $Ins(1,4,5)P_3$ receptor antisense cDNA prevented specific TCR-mediated IL-2 production and cell proliferation [10], indicating that impairment of $Ca^{2+}$ mobilization affects the proliferative capacity of T-lymphocytes. Similarly, antisense-induced knockdown of CHERP in HEL cells was associated not only with reduced $Ca^{2+}$ mobilization, but also with decreased cell proliferation and a marked increase of cells displaying a marker for senescense [1]. Figure 5 shows a typical experiment in which the overall proliferation of AS-Jurkat cells incubated with IPTG was decreased by approx. 75 %, compared with control AS-Jurkat cells (minus IPTG), over a period of 96 h. During the last 48 h with IPTG, the number of CHERP-depleted cells barely increased. The viability of the IPTG-treated AS-Jurkat cells, measured by Trypan

Blue exclusion, ranged from 92–97 % over the 96 h period, which was no different from that of AS-Jurkat cells in the absence of IPTG. There was no increase in the senescence marker enzyme $\beta$-galactosidase [26], nor in apoptotic cells measured by a TUNEL assay, in either population of cells (results not shown). Therefore decreased viability does not account for the magnitude of the decline in cell proliferation in CHERP-depleted cells.

We concluded that the decrease in the rate of proliferation was attributable to delays in the transit of cells through the cell cycle, or arrest of the cycle in a substantial fraction of the cells. Therefore, cyclin D1 levels were measured in AS-Jurkat cells incubated with IPTG. Cyclin D1 is normally elevated when cells are stimulated by growth factors to enter the cell cycle, and is necessary for progression through the $G_1$ phase of the cycle, thereby regulating cell proliferation [36]. The concentration of cyclin D1, measured by immunofluorescence microscopy in 108 cells, was significantly decreased after treatment of AS-Jurkat cells with IPTG. Cyclin D1 decreased by 40 % after 24 h and 63.4 % after 48 h with IPTG; i.e. $F_{mean}=1.58\pm0.21$ in 42 IPTG-treated cells, compared with $F_{mean}=4.30\pm0.38$ in 44 untreated cells at 48 h. The difference between time zero and 48 h was statistically significant ($P<0.01$).

**Serum deprivation increases CHERP concentration in Jurkat cells**

Serum withdrawal, which causes cultured cells in the $G_1$ phase of the cell cycle to exit into the non-dividing $G_0$ state [37], arrested proliferation of HEL cells, but caused a large increase of CHERP concentration (F. A. O'Rourke and M. B. Feinstein, unpublished work). Wild-type Jurkat cells growing in RPMI 1640 medium containing 10 % (v/v) FBS were washed and resuspended in RPMI 1640 without serum. Some cells, initially incubated without serum for 72 h at 37 °C, were returned to medium containing serum for an additional 72 h. For each experimental condition, cells were processed for the measurement of CHERP and other proteins [RNA polymerase II, cyclin D1 and the $Ins(1,4,5)P_3$ receptor] by immunofluorescence microscopy. In serum-free medium, the proliferation of wild-type Jurkat cells was arrested for about 4 days, after which the cells resumed growth and formed large ball-like floating aggregates, visible to the naked eye. In two separate experiments, withdrawal of serum for 72 h had no significant effect on the content of the $Ins(1,4,5)P_3$ receptor or cyclin D1, but caused a mean 4.67-fold increase in CHERP immunofluorescence (ratio of $F_{mean}=28/6$; $n=69$ without serum and $n=75$ with serum; $P<0.05$) that was totally reversed by restoring serum to the culture medium. The largest subunit of RNA polymerase II, measured using an antibody against its C-terminal domain (CTD), increased 3-fold after withdrawal of serum. RNA polymerase II is the key enzyme for mRNA transcription, and the CTD is important for recruiting many of the other nuclear proteins that are part of the transcriptional machinery [38].

The initial arrest of cell proliferation due to absence of serum provided an opportunity to compare $Ca^{2+}$ mobilization in those cells with that in non-proliferating CHERP-depleted cells, to determine if lack of proliferation could account for decreased $Ca^{2+}$ mobilization in the latter case. Serum deprivation for 72 h did not inhibit the rise of $[Ca^{2+}]_i$ due to PHA or thrombin (results not shown). The steady-state peak rise of $[Ca^{2+}]_i$ caused by the SERCA inhibitor cyclopiazonic acid in six batches of cells incubated without serum was greater than in three of five batches of cells in serum. However, the difference in the mean increases in $[Ca^{2+}]_i$ in the two groups was not statistically significant ($0.59\pm0.1$ $\mu$M in serum compared with $0.75\pm0.076$ $\mu$M in the absence of serum; $P=0.22$). The rate of increase of $[Ca^{2+}]_i$ induced by cyclopiazonic acid was greater in all batches of serum-deprived cells, suggesting that those cells with increased CHERP

content have normal or somewhat increased ER Ca$^{2+}$ stores than cells maintained in serum.

## DISCUSSION

The principal finding of our experiments is that an antisense-mediated knockdown of CHERP impaired the ability of Jurkat cells to increase [Ca$^{2+}$]$_i$ in response to activation by PHA or thrombin. There was a direct relationship between the extent of the depletion of CHERP in AS-Jurkat cells and the loss of the Ca$^{2+}$-mobilizing effect of PHA. In cells that lost > 70 % of CHERP, the mitogen PHA increased [Ca$^{2+}$]$_i$ by $\leqslant$ 30 % of the response in control cells. Cells with decreased geniticin resistance and response to IPTG lost only approx. 50 % of CHERP, and their response to PHA was greater, but still less than normal. These findings suggest that there is not a great excess of CHERP in Jurkat cells, with respect to its role in Ca$^{2+}$ homoeostasis. The reduced mobilization of Ca$^{2+}$ in CHERP-depleted cells could be due to defective signal transduction leading to the production of Ins(1,4,5)$P_3$, but that is unlikely since each agonist activates a different signalling pathway. Other possible mechanisms include impaired response to Ins(1,4,5)$P_3$ [although the concentration of Ins(1,4,5)$P_3$ receptors was unaffected], a decrease of ER Ca$^{2+}$ stores or a defective Ca$^{2+}$ influx, or any combination of these factors.

Inhibition of SERCA by thapsigargin causes release of Ca$^{2+}$ directly from ER stores, which leads to an influx of extracellular Ca$^{2+}$, largely, if not entirely, through CRAC channels. A loss of approx. 50 % of CHERP significantly reduced the response to PHA, but had no effect on PHA-induced Ca$^{2+}$ influx or the response to thapsigargin. In contrast, IPTG-treated AS-Jurkat cells with the most severe loss of CHERP (>70 %) and of the response to PHA had decreased Ca$^{2+}$ influx and a partially impaired rate of rise of [Ca$^{2+}$]$_i$ in response to thapsigargin. However, the increase of [Ca$^{2+}$]$_i$ elicited by thapsigargin was much larger than the response to PHA, indicating that the Ins(1,4,5)$P_3$-dependent pathway for Ca$^{2+}$ release from the ER was the parameter most affected by the loss of CHERP. This conclusion is in accord with our previous finding of the inhibition of Ins(1,4,5)$P_3$-induced Ca$^{2+}$ release from ER membrane vesicles by a monoclonal antibody against CHERP, and with the defective response to thrombin in HEL cells with an antisense-mediated knockdown of CHERP [1,3]. Our findings also indicate that severe loss of CHERP in the lymphocyte line affects not only the mobilization of ER Ca$^{2+}$ by PHA (and thrombin), but also the magnitude of the ER Ca$^{2+}$ stores and/or the mechanism for the influx of Ca$^{2+}$ through SOCs.

Although the mechanism by which depletion of ER Ca$^{2+}$ stores leads to influx of extracellular Ca$^{2+}$, and the nature of the channel(s) through which Ca$^{2+}$ flows, are far from settled issues [39–41], the direct relationship between store depletion and the magnitude of CRAC has been deduced indirectly [28,41]. It is also supported by more direct measurements made by Hofer et al. [42] in RBL-1 cells. The latter investigators simultaneously measured ER Ca$^{2+}$ stores with Mag-fura-2/AM fluorescence and $I_{CRAC}$ by whole cell clamping. The membrane-permeant chelator $N,N,N',N'$-tetrakis-(2-pyridylmethyl)ethylenediamine ('TPEN') produced a dose-dependent decrease of Ca$^{2+}$ stores in the ER and a concurrent graded decrease of $I_{CRAC}$ in proportion to the decrease of ER Ca$^{2+}$ store concentration. These data suggest that a deficiency of ER Ca$^{2+}$ stores in AS-Jurkat cells could account for the decreased response to SERCA inhibitors and decreased Ca$^{2+}$ influx through SOCs that we observed in severely CHERP-depleted cells. There is no known role for CHERP in

regulating ER Ca$^{2+}$ stores, and our results in Jurkat cells differ from those in HEL cells. A substantial depletion of CHERP in HEL cells, although severely decreasing Ca$^{2+}$ mobilization by thrombin, had no significant effect on thapsigargin-releasable ER Ca$^{2+}$ stores or on CRAC, measured indirectly [1]. Thus, in HEL cells, the loss of CHERP is associated solely with a defect in the mobilization of Ca$^{2+}$ from the stores, which is Ins(1,4,5)$P_3$-dependent. Jurkat cells differ from HEL cells in their rapid loss of ER stores in Ca$^{2+}$-free media or in the presence of Ca$^{2+}$-channel blockers [13]. Thus differences in the ability of these two cells types to maintain their ER Ca$^{2+}$ stores may account for the differences we observed between the two cell types when CHERP was depleted. Subsequent detailed studies to measure ER stores and $I_{CRAC}$ directly in CHERP-depleted cells are necessary to settle these issues.

Regardless of the mechanism(s) by which loss of CHERP impairs Ca$^{2+}$ mobilization, the downstream effects on Ca$^{2+}$-dependent processes, such as activation of NFAT and cellular proliferation, are clear. The activation and translocation of the transcription factor NFAT to the nucleus of T-cells is necessary for the production of IL-2 and for clonal expansion of antigen-stimulated cells. A rise of T-cell [Ca$^{2+}$]$_i$ activates the Ca$^{2+}$/calmodulin-dependent phosphatase calcineurin, which substantially dephosphorylates cytoplasmic NFAT [43], exposing a nuclear localization sequence in the protein that permits its transfer into the nucleus [44,45]. Sustained influx of Ca$^{2+}$ is necessary to maintain NFAT in the nucleus, since a fall of [Ca$^{2+}$]$_i$ results in its rapid rephosphorylation [46] and export from the nucleus [44]. The activation and translocation of NFAT1 to the nucleus of AS-Jurkat cells was blocked, as expected, by the calcineurin antagonist cyclosporin and by chelation of extracellular Ca$^{2+}$. AS-Jurkat cells treated with IPTG to deplete CHERP also had greatly reduced ability to translocate NFAT to the nucleus, an effect that was clearly due to the failure of those cells to mobilize Ca$^{2+}$, because it was totally overcome by the addition of the Ca$^{2+}$ ionophore ionomycin. This clearly demonstrates the need for CHERP in an important T-cell Ca$^{2+}$-dependent biochemical response, and implies that the loss of CHERP content or function could adversely affect immune system functions.

Cell proliferation is another Ca$^{2+}$-regulated biological process affected by CHERP. In HEL cells, the loss of CHERP decreased the incorporation of thymidine into DNA, arrested cell proliferation, and increased an enzyme marker for senescence [1]. In Jurkat cells, the antisense-mediated knockdown of CHERP also caused a marked decline in cell proliferation, without loss of viability, increased apoptosis or evidence of senescence. It was accompanied by a substantial decline in cyclin D1 concentration, and the greatest slowing of proliferation occurred when the cyclin D1 levels were at their lowest level. Cyclin D1 is necessary for cell-cycle progression through G$_1$ into S phase. Overexpression or excessive activity of cyclin D1 is found in many human tumours [47] and causes a malignant phenotype in normal cells [48], whereas suppression of cyclin D1 can reverse a malignant phenotype [49,50].

Several reported observations suggest that the slowed proliferation and decrease in cyclin D1 that we observed in IPTG-treated AS-Jurkat cells may be directly related to the depletion of CHERP and the ensuing impairment of Ca$^{2+}$ homoeostasis. Cell-cycle progression is inhibited by loss of SERCA activity and ER Ca$^{2+}$ [51], and defective Ca$^{2+}$ homoeostasis appears to prevent cyclin D1 expression during G$_1$. Inactivation of SERCA caused G$_0$/G$_1$ arrest or lengthening of the G$_1$ phase in C6 glioma and HEK-293 cells, along with reduced cyclin D1 and other cell-cycle regulators [52]. In NIH3T3 cells, the drug clotrimazole released internal Ca$^{2+}$ stores and also blocked subsequent store-regulated

Ca$^{2+}$ influx, resulting in depletion of internal Ca$^{2+}$, inhibition of cyclin D1 synthesis at the level of translation, and inhibition of growth [53]. Similarly, serum-stimulated human fibroblasts could not progress through the G$_1$/S boundary when Ca$^{2+}$ stores were depleted by thapsigargin [54]. These findings in various cell types suggest that the internal Ca$^{2+}$ store is an important regulator of the synthesis of cyclin D1 and of the G$_1$ phase of the cell cycle. Our findings suggest that CHERP is a component of the system that directly or indirectly regulates cyclin D1 levels and cell proliferation, although the exact mechanisms by which it does so remain unknown. In addition, it appears that CHERP has a permissive role in the rapid proliferation of the leukaemic cell lines HEL and Jurkat.

Since the concentration of CHERP affects Ca$^{2+}$-dependent processes, we began to study other conditions that might regulate expression of the protein. Withdrawal of serum from the culture medium caused a large increase of CHERP in HEL cells (F. A. O'Rourke and M. B. Feinstein, unpublished work) and a $> 4$-fold increase in Jurkat cells. The latter was accompanied by an increase of the major subunit of RNA polymerase II that is a key part of the eukaryotic protein machine for transcribing DNA into RNA. CHERP concentration may be regulated in concert with a number of genes identified in different systems that are induced by serum starvation and down-regulated by the addition of serum, suggesting that they have a role in cell-growth control [55]. Jurkat cells that were initially growth-arrested by serum deprivation, with elevated CHERP, had no deficit in Ca$^{2+}$ mobilization by PHA, and they responded as well or slightly better to SERCA inhibitors than cells in serum, suggesting that the ER Ca$^{2+}$ stores in those cells were normal or somewhat larger, or better coupled to CRAC. Finally, those findings argue against attributing defective Ca$^{2+}$ mobilization in CHERP-depleted cells to the concomitant arrest of cell proliferation. Serum-deprived Jurkat cells were equally growth-arrested for a period of time, during which they had elevated CHERP and normal or enhanced Ca$^{2+}$ mobilization. Therefore the inability of PHA and thrombin to mobilize Ca$^{2+}$ in IPTG-treated AS-Jurkat cells was unlikely to be a consequence of arrested proliferation, but rather a consequence of the loss of CHERP.

## REFERENCES

1  LaPlante, J. M., O'Rourke, F., Lu, X., Fein, A., Olsen, A. and Feinstein, M. B. (2000) Cloning of human Ca$^{2+}$ homoeostasis endoplasmic reticulum protein (CHERP): regulated expression of antisense cDNA depletes CHERP, inhibits intracellular Ca$^{2+}$ mobilization and decreases cell proliferation. Biochem. J. **348**, 189–199

2  Imbert, G., Saudou, F., Yvert, G., Devys, D., Trottier, Y., Garnier, J. M., Weber, C., Mandel, J. L., Cancel, G., Abbas, N. et al. (1996) Cloning of the gene for spinocerebellar ataxia 2 reveals a locus with high sensitivity to expanded CAG/glutamine repeats. Nat. Genet. **14**, 285–291

3  O'Rourke, F., Soons, K., Flaumenhauft, R., Watras, J., Baio-Larue, C., Matthews, E. and Feinstein, M. B. (1994) Ca$^{2+}$ release by inositol 1,4,5-trisphosphate is blocked by the K$^+$-channel blockers apamin and tetrapentylammonium ion, and a monoclonal antibody to a 63 kDa membrane protein: reversal of blockade by K$^+$ ionophores nigericin and valinomycin and purification of the 63 kDa antibody-binding protein. Biochem. J. **300**, 673–683

4  Muallem, S., Schoeffield, M., Pandol, S. and Sachs, G. (1985) Inositol trisphosphate modification of ion transport in rough endoplasmic reticulum. Proc. Natl. Acad. Sci. U.S.A. **82**, 4433–4437

5  Nguyen, T., Chin, W. C. and Verdugo, P. (1998) Role of Ca$^{2+}$/K$^+$ ion exchange in intracellular storage and release of Ca$^{2+}$. Nature (London) **395**, 908–912

6  Treves, S., Di Virgilio, F., Cerundolo, V., Zanovello, P., Collavo, D. and Pozzan, T. (1987) Calcium and inositol phosphates in the activation of T cell-mediated cytotoxicity. J. Exp. Med. **166**, 33–42

7  Ransom, J. T., Harris, L. K. and Cambier, J. C. (1986) Anti-Ig induces release of inositol 1,4,5-trisphosphate, which mediates mobilization of intracellular Ca$^{++}$ stores in B lymphocytes. J. Immunol. **137**, 708–714

8  Le Deist, F., Hivroz, C., Partiseti, M., Thomas, C., Buc, H. A., Oleastro, M., Belohradsky, B., Choquet, D. and Fischer, A. (1995) A primary T-cell immunodeficiency associated with defective transmembrane calcium influx. Blood **85**, 1053–1062

9  Partiseti, M., Le Deist, F., Hivroz, C., Fischer, A., Korn, H. and Choquet, D. (1994) Defective transmembrane calcium influx demonstrated in a primary immunodeficiency by video-imaging. C. R. Acad. Sci. Ser. III **317**, 167–173

10  Jayaraman, T., Ondriasova, E., Ondrias, K., Harnick, D. J. and Marks, A. R. (1995) The inositol 1,4,5-trisphosphate receptor is essential for T-cell receptor signaling. Proc. Natl. Acad. Sci. U.S.A. **92**, 6007–6011

11  Fanger, C. M., Hoth, M., Crabtree, G. R. and Lewis, R. S. (1995) Characterization of T cell mutants with defects in capacitative calcium entry: genetic evidence for the physiological roles of CRAC channels. J. Cell Biol. **131**, 655–667

12  Dellis, O., Gangloff, S. C., Paulais, M., Tondelier, D., Rona, J. P., Brouillard, F., Bouteau, F., Guenounou, M. and Teulon, J. (2002) Inhibition of the calcium release-activated calcium (CRAC) current in Jurkat T cells by the HIV-1 envelope protein gp160. J. Biol. Chem. **277**, 6044–6050

13  Lewis, R. S. (2001) Calcium signaling mechanisms in T lymphocytes. Annu. Rev. Immunol. **19**, 497–521

14  Dolmetsch, R. E., Lewis, R. S., Goodnow, C. C. and Healy, J. I. (1997) Differential activation of transcription factors induced by Ca$^{2+}$ response amplitude and duration. Nature (London) **386**, 855–858

15  Gardner, P. (1989) Calcium and T lymphocyte activation. Cell **59**, 15–20

16  Putney, Jr, J. W. (1986) A model for receptor-regulated calcium entry. Cell Calcium **7**, 1–12

17  Hohenegger, M., Berg, I., Weigl, L., Mayr, G. W., Potter, B. V. and Guse, A. H. (1999) Pharmacological activation of the ryanodine receptor in Jurkat T-lymphocytes. Br. J. Pharmacol. **128**, 1235–1240

18  Takeshima, H., Ikemoto, T., Nishi, M., Nishiyama, N., Shimuta, M., Sugitani, Y., Kuno, J., Saito, I., Saito, H., Endo, M. et al. (1996) Generation and characterization of mutant mice lacking ryanodine receptor type 3. J. Biol. Chem. **271**, 19649–19652

19  Dolmetsch, R. E., Xu, K. and Lewis, R. S. (1998) Calcium oscillations increase the efficiency and specificity of gene expression. Nature (London) **392**, 933–936

20  Waldmann, T. A., Goldman, C. K., Robb, R. J., Depper, J. M., Leonard, W. J., Sharrow, S. O., Bongiovanni, K. F., Korsmeyer, S. J. and Greene, W. C. (1984) Expression of interleukin 2 receptors on activated human B cells. J. Exp. Med. **160**, 1450–1466

21  Henney, C. S., Kuribayashi, K., Kern, D. E. and Gillis, S. (1981) Interleukin-2 augments natural killer cell activity. Nature (London) **291**, 335–338

22  Rao, A., Luo, C. and Hogan, P. G. (1997) Transcription factors of the NFAT family: regulation and function. Annu. Rev. Immunol. **15**, 707–747

23  Lu, X., Fein, A., Feinstein, M. B. and O'Rourke, F. A. (1999) Antisense knock out of the inositol 1,3,4,5-tetrakisphosphate receptor GAP1$^{IP4BP}$ in the human erythroleukemia cell line leads to the appearance of intermediate conductance K(Ca) channels that hyperpolarize the membrane and enhance calcium influx. J. Gen. Physiol. **113**, 81–96

24  Tsien, R. Y., Rink, T. J. and Poenie, M. (1985) Measurement of cytosolic free Ca$^{2+}$ in individual small cells using fluorescence microscopy with dual excitation wavelengths. Cell Calcium **6**, 145–157

25  Grynkiewicz, G., Poenie, M. and Tsien, R. Y. (1985) A new generation of Ca$^{2+}$ indicators with greatly improved fluorescence properties. J. Biol. Chem. **260**, 3440–3450

26  Dimri, G. P., Lee, X., Basile, G., Acosta, M., Scott, G., Roskelley, C., Medrano, E. E., Linskens, M., Rubelj, I., Pereira-Smith, O. et al. (1995) A biomarker that identifies senescent human cells in culture and in aging skin in vivo. Proc. Natl. Acad. Sci. U.S.A. **92**, 9363–9367

27  Mari, B., Imbert, V., Belhacene, N., Far, D. F., Peyron, J.-F., Pouyssgur, J., Van Obberghen-Schilling, E., Rossi, B. and Auberger, P. (1994) Thrombin and thrombin receptor agonist peptide induce early events of T cell activation and synergize with TCR cross-linking for CD69 expression and interleukin 2 production. J. Biol. Chem. **269**, 8517–8523

28  Zweifach, A. and Lewis, R. S. (1993) Mitogen-regulated Ca$^{2+}$ current of T lymphocytes is activated by depletion of intracellular Ca$^{2+}$ stores. Proc. Natl. Acad. Sci. U.S.A. **90**, 6295–6299

29  Zweifach, A. and Lewis, R. S. (1996) Calcium-dependent potentiation of store-operated calcium channels in T lymphocytes. J. Gen. Physiol. **107**, 597–610

30 Donnadieu, E., Bismuth, G. and Trautmann, A. (1992) Calcium fluxes in T lymphocytes. J. Biol. Chem. **267**, 25864–25872

31 Fischer, B. S., Qin, D., Kim, K. and McDonald, T. V. (2001) Capsaicin inhibits Jurkat T-cell activation by blocking calcium entry current $I_{CRAC}$. J. Pharmacol. Exp. Ther. **299**, 238–246

32 Fomina, A. F., Fanger, C. M., Kozak, J. A. and Cahalan, M. D. (2000) Single channel properties and regulated expression of Ca$^{2+}$ release-activated Ca$^{2+}$ (CRAC) channels in human T cells. J. Cell Biol. **150**, 1435–1444

33 Gardner, P. (1990) Patch clamp studies of lymphocyte activation. Annu. Rev. Immunol. **8**, 231–252

34 Partiseti, M., Le Deist, F., Hivroz, C., Fischer, A., Korn, H. and Choquet, D. (1994) The calcium current activated by T cell receptor and store depletion in human lymphocytes is absent in a primary immunodeficiency. J. Biol. Chem. **269**, 32327–32335

35 Murphy, L. L. and Hughes, C. C. (2002) Endothelial cells stimulate T cell NFAT nuclear translocation in the presence of cyclosporin A: involvement of the wnt/glycogen synthase kinase-3$\beta$ pathway. J. Immunol. **169**, 3717–3725

36 Yu, B., Lane, M. E., Pestell, R. G., Albanese, C. and Wadler, S. (2000) Downregulation of cyclin D1 alters cdk 4- and cdk 2-specific phosphorylation of retinoblastoma protein. Mol. Cell. Biol. Res. Commun. **3**, 352–359

37 Iyer, V. R., Eisen, M. B., Ross, D. T., Schuler, G., Moore, T., Lee, J. C., Trent, J. M., Staudt, L. M., Hudson, Jr, J., Boguski, M. S. et al. (1999) The transcriptional program in the response of human fibroblasts to serum. Science **283**, 83–87

38 Howe, K. (2002) RNA polymerase II conducts a symphony of pre-mRNA processing activities. Biochim. Biophys. Acta **1577**, 308–324

39 Putney, Jr, J. W., Broad, L. M., Braun, F. J., Lievremont, J. P. and Bird, G. S. (2001) Mechanisms of capacitative calcium entry. J. Cell Sci. **114**, 2223–2229

40 Clapham, D. E. (2002) Sorting out MIC, TRP, and CRAC ion channels. J. Gen. Physiol. **120**, 217–220

41 Krause, E., Schmid, A., Gonzalez, A. and Schulz, I. (1999) Low cytoplasmic [Ca$^{2+}$] activates $I_{CRAC}$ independently of global Ca$^{2+}$ store depletion in RBL-1 cells. J. Biol. Chem. **274**, 36957–36962

42 Hofer, A. M., Fasolato, C. and Pozzan, T. (1998) Capacitative Ca$^{2+}$ entry is closely linked to the filling state of internal Ca$^{2+}$ stores: a study using simultaneous measurements of $I_{CRAC}$ and intraluminal [Ca$^{2+}$]. J. Cell Biol. **140**, 325–334

43 Ruff, V. A. and Leach, K. L. (1995) Direct demonstration of NFATp dephosphorylation and nuclear localization in activated HT-2 cells using a specific NFATp polyclonal antibody. J. Biol. Chem. **270**, 22602–22607

44 Luo, C., Shaw, K. T., Raghavan, A., Aramburu, J., Garcia-Cozar, F., Perrino, B. A., Hogan, P. G. and Rao, A. (1996) Interaction of calcineurin with a domain of the transcription factor NFAT1 that controls nuclear import. Proc. Natl. Acad. Sci. U.S.A. **93**, 8907–8912

45 Okamura, H., Aramburu, J., Garcia-Rodriguez, C., Viola, J. P., Raghavan, A., Tahiliani, M., Zhang, X., Qin, J., Hogan, P. G. and Rao, A. (2000) Concerted dephosphorylation of the transcription factor NFAT1 induces a conformational switch that regulates transcriptional activity. Mol. Cell **6**, 539–550

46 Gomez del Arco, P., Martinez-Martinez, S., Maldonado, J. L., Ortega-Perez, I. and Redondo, J. M. (2000) A role for the p38 MAP kinase pathway in the nuclear shuttling of NFATp. J. Biol. Chem. **275**, 13872–13878

47 Peters, G. (1994) The D-type cyclins and their role in tumorigenesis. J. Cell Sci. Suppl. **18**, 89–96

48 Jiang, W., Kahn, S. M., Zhou, P., Zhang, Y. J., Cacace, A. M., Infante, A. S., Doi, S., Santella, R. M. and Weinstein, I. B. (1993) Overexpression of cyclin D1 in rat fibroblasts causes abnormalities in growth control, cell cycle progression and gene expression. Oncogene **8**, 3447–3457

49 Sherr, C. J., Kato, J., Quelle, D. E., Matsuoka, M. and Roussel, M. F. (1994) D-type cyclins and their cyclin-dependent kinases: G1 phase integrators of the mitogenic response. Cold Spring Harbor Symp. Quant. Biol. **59**, 11–19

50 Sherr, C. J. (1995) D-type cyclins. Trends Biochem. Sci. **20**, 187–190

51 Simon, V. R. and Moran, M. F. (2001) SERCA activity is required for timely progression through G$_1$/S. Cell Proliferation **34**, 15–30

52 Chen, Y. J., Lin, J. K. and Lin-Shiau, S. Y. (1999) Proliferation arrest and induction of CDK inhibitors p21 and p27 by depleting the calcium store in cultured C6 glioma cells. Eur. J. Cell Biol. **78**, 824–831

53 Aktas, H., Fluckiger, R., Acosta, J. A., Savage, J. M., Palakurthi, S. S. and Halperin, J. A. (1998) Depletion of intracellular Ca$^{2+}$ stores, phosphorylation of eIF2$\alpha$, and sustained inhibition of translation initiation mediate the anticancer effects of clotrimazole. Proc. Natl. Acad. Sci. U.S.A. **95**, 8280–8285

54 Takuwa, N., Zhou, W., Kumada, M. and Takuwa, Y. (1995) Involvement of intact inositol-1,4,5-trisphosphate-sensitive Ca$^{2+}$ stores in cell cycle progression at the G$_1$/S boundary in serum-stimulated human fibroblasts. FEBS Lett. **360**, 173–176

55 Schneider, C., King, R. M. and Philipson, L. (1988) Genes specifically expressed at growth arrest of mammalian cells. Cell **54**, 787–793